

Controllable Chemical Vapor Deposition Growth of Few Layer Graphene for Electronic Devices

DACHENG WEI,^{†,‡} BIN WU,[†] YUNLONG GUO,[†] GUI YU,[†] AND
YUNQI LIU^{*,†}

[†]Beijing National Laboratory for Molecular Sciences, Key Laboratory of Organic Solids, Institute of Chemistry, Chinese Academy of Sciences, Beijing 100190, People's Republic of China, and [‡]Physics Department, National University of Singapore, 2 Science Drive 3, Singapore 117542

RECEIVED ON APRIL 5, 2012

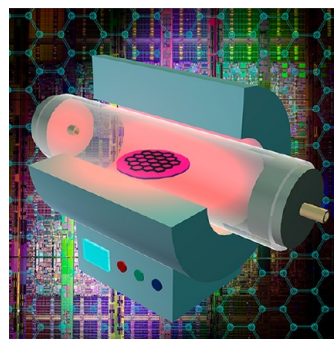
CONSPECTUS

Because of its atomic thickness, excellent properties, and widespread applications, graphene is regarded as one of the most promising candidate materials for nanoelectronics. The wider use of graphene will require processes that produce this material in a controllable manner. In this Account, we focus on our recent studies of the controllable chemical vapor deposition (CVD) growth of graphene, especially few-layer graphene (FLG), and the applications of this material in electronic devices.

CVD provides various means of control over the morphologies of the produced graphene. We studied several variables that can affect the CVD growth of graphene, including the catalyst, gas flow rate, growth time, and growth temperature and successfully achieved the controlled growth of hexagonal graphene crystals. Moreover, we developed several modified CVD methods for the controlled growth of FLGs. Patterned CVD produced FLGs with desired shapes in required areas. By introducing dopant precursor in the CVD process, we produced substitutionally doped FLGs, avoiding the typically complicated post-treatment processes for graphene doping. We developed a template CVD method to produce FLG ribbons with controllable morphologies on a large scale. An oxidation-activated surface facilitated the CVD growth of polycrystalline graphene without the use of a metal catalyst or a complicated postgrowth transfer process.

In devices, CVD offers a controllable means to modulate the electronic properties of the graphene samples and to improve device performance. Using CVD-grown hexagonal graphene crystals as the channel materials in field-effect transistors (FETs), we improved carrier mobility. Substitutional doping of graphene in CVD opened a band gap for efficient FET operation and modulated the Fermi energy level for n-type or p-type features. The similarity between the chemical structure of graphene and organic semiconductors suggests potential applications of graphene in organic devices. We used patterned CVD FLGs as the bottom electrodes in pentacene FETs. The strong π - π interactions between graphene and pentacene produced an excellent interface with low contact resistance and a reduced injection barrier, which dramatically enhances the device performance. We also fabricated reversible nanoelectromechanical (NEM) switches and a logic gate using the FLG ribbons produced using our template CVD method.

In summary, CVD provides a controllable means to produce graphene samples with both large area and high quality. We developed several modified CVD methods to produce FLG samples with controlled shape, location, edge, layer, dopant, and growth substrate. As a result, we can modulate the properties of FLGs, which provides materials that could be used in FETs, OFETs, and NEM devices. Despite remarkable advances in this field, further exploration is required to produce consistent, homogeneous graphene samples with single layer, single crystal, and large area for graphene-based electronics.



1. Introduction

Graphene, the first example of free-standing two-dimensional (2D) crystals,¹ has attracted an enormous amount of interest from both theoretical and experimental scientists, although intensive research on graphene only began in

2004,² because this material combines excellent mechanical and electronic properties with atomic thickness.^{3,4} Electrons in graphene obey a linear dispersion relationship and behave as Dirac fermions with zero effective mass, which gives rise to extraordinary electronic properties like

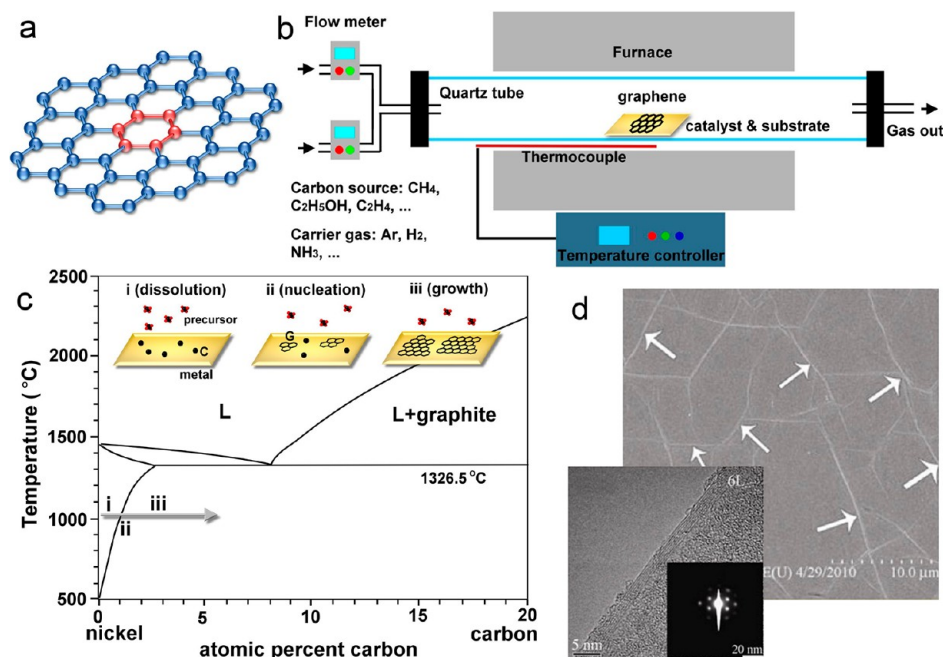


FIGURE 1. (a) Molecular structure of graphene, which can be obtained by deductively extending a benzene ring (red) in 2D. (b) Schematics of the CVD system for graphene growth. (c) The binary phase diagram of nickel and carbon, with an indication of the compositional zones responsible for (i) dissolution, (ii) nucleation, and (iii) growth. (d) SEM image of FLGs produced by Fe-catalyzed CVD with wrinkles marked by arrows. The inset shows the TEM image and electron diffraction pattern of the FLGs. Reproduced with permission from ref 16. Copyright 2011 Tsinghua University Press and Springer-Verlag GmbH.

the absence of charge localization, half-integer quantum Hall effect, ultrahigh mobility, and charge concentration.⁵ Its room-temperature mobility is predicted to be as high as $200\,000\text{ cm}^2\text{ V}^{-1}\text{ s}^{-1}$,⁶ orders of magnitude higher than that of modern Si transistors, while its room-temperature ballistic transport distance is up to micrometer scale in the presence of substrate-induced disorder;⁷ therefore, graphene is usually considered as one promising candidate for future nanoelectronics and holds great promise for widespread applications like field-effect transistors (FETs), sensors, supercapacitors, nanocomposites, solar cells, electrode materials, etc.^{1,2,5,6,8}

Graphene has a distinct structure from three-dimensional (3D) diamond and is the basic building block for graphitic materials of all other dimensionalities.^{1,5} It consists of sp^2 -bonded carbon atoms, which are tightly packed into an atomically thick layer of honeycomb lattice; thus it can be considered as a type of material obtained by deductively extending a benzene ring in two dimensions (Figure 1a). Different arrangement of benzene rings in the 2D space results in graphene sheets with various morphologies, while different covalent bonding with other atoms results in different modifications of the graphene sheets, causing the existence of graphene materials with various properties.⁹ Therefore, as the first step for practical applications, graphene must be synthesized in a controllable manner. Till

now, methods like mechanical exfoliation, chemical exfoliation of graphite oxide, arc-discharge, epitaxial growth such as chemical vapor deposition (CVD), and thermal decomposition of SiC were developed to produce graphene.^{3,4,9,10} However, the present synthetic methods usually suffer from limited controllability over the size, shape, edge, location, doping or layer structure of graphene due to the random exfoliation, growth, or assembly process. Comparatively, CVD offers a relatively controllable means to produce graphene samples with large area and high quality,^{4,10} both of which are also of great importance for practical applications; thus our interest has been focused here recently, specially on the controllable CVD growth of few-layer graphene (FLG), which has special applications and is of scientific as well as technological importance similar to single-layer graphene.^{11,12} Our research attempts to find the routes to control the CVD growth of graphene and then to produce FLG samples with required properties for various device applications. In this Account, we review our recent efforts toward this goal and discuss several modified CVD techniques in detail.

2. Controllable Chemical Vapor Deposition of Few-Layer Graphene

2.1. Chemical Vapor Deposition.

CVD is a process in which gaseous precursors are reactively transformed into a

thin film, coating, or other solid-state material on the surface of a catalyst or substrate. It is widely used in the semiconductor industry and also in controllable growth of nanomaterials like nanowires, carbon nanotubes, etc.^{10,13} The CVD growth of graphitic materials on transition metal surfaces such as Co, Pt, Ir, Ru, and Ni has been well-known since the 1990s or earlier.^{4,10,14,15} Till now, CVD has become one of the most important commercial methods for graphene production, because it can be easily scaled to industrial production levels.¹⁰ Figure 1b depicts a schematic experimental setup for CVD of graphene. The growth process involves heating the catalyst to high temperatures in a tube furnace and flowing gaseous or volatile compounds of carbon as the precursor through the tube reactor. At high temperature, the hydrocarbon molecules catalytically decompose and then dissolve in catalyst. According to the phase diagram (i.e., C–Ni, Figure 1c), the nucleation and then the growth of graphitic carbon layers from the saturated catalyst surface take place by means of precipitation, as a result of continuously feeding precursor molecules. Finally, the enlargement of graphene grains connects them into a continuous membrane over the catalyst. Figure 1d shows a FLG film produced by an ambient-pressure CVD process using 100 μm Fe foils as the catalyst.¹⁶ After pyrolysis of CH_4 at 920 $^\circ\text{C}$, the whole foil was covered by a continuous FLG film with wrinkles. The unobvious D-band of the Raman spectra and symmetric hexagonal spots in electron diffraction patterns revealed a good quality and an AB stacking of the graphene layers. The sizes of FLG are determined by the Fe foil; thus it has the potential for further increasing by using larger Fe foils.

2.2. Controllability of Chemical Vapor Deposition. It is well known that many factors, such as hydrocarbon, catalyst, gas flow, pressure, growth time, growth temperature, and cooling rate, play distinct roles in the CVD process, leading to various morphologies of the produced graphene. At the same time, these factors also provide us effective means to control the growth. For instance, catalyst type can influence the properties of the as-grown graphene like quality, continuity, and layer number distribution, due to the different growth mechanisms and solubilities of carbon. Ni catalysts usually produce nonuniform FLG films,¹⁵ while Cu catalysts result in single-layer graphene under low pressure conditions due to the ultralow carbon solubility and the surface-related growth mechanism.^{10,14} We produced high-quality FLG films on Fe, which is favorable for low-cost and easy etching.¹⁶ Here, we detail the controllability of CVD by using our recent work on hexagonal graphene as an

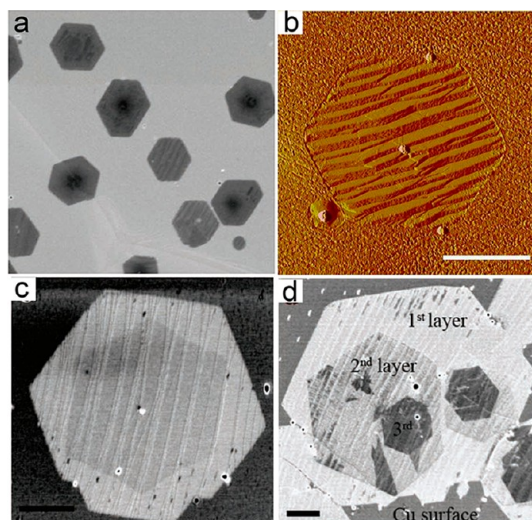


FIGURE 2. (a) SEM image and (b) AFM image of the hexagonal graphene (produced by pyrolysis of 10/300 sccm CH_4/H_2 on copper foil at 1000 $^\circ\text{C}$ for 40 min). (c, d) SEM images of FLGs stacked by (c) two hexagonal layers with 30 $^\circ$ rotation, and (d) three hexagonal layers.¹⁷ Copyright 2011 Wiley Publishers.

instance.¹⁷ The hexagonal graphene was produced by pyrolysis of CH_4 on Cu foils at ambient pressure (Figure 2a,b). The edges appear as straight and smooth lines with angles of 120 $^\circ$. The unique shape of graphene is strongly indicative of a single crystalline structure with either zigzag or armchair edges. The absence of D-band in the Raman spectra reveals the high quality of the crystalline structure, which is of great significance for the electrical applications of graphene. The evolution of the size, shape, and density of hexagonal graphene was studied by varying certain factors. Both the average size and density monotonically increased with growth time, while shape remained unchanged. The nucleation of graphene was modulated by the crystallinity, defect, grain size, and grain density of the Cu surface, and lower graphene domain densities could be obtained by annealing Cu for a longer time. The morphology and perfection of geometric structure of graphene were strongly dependent on CH_4 flow rates. Higher CH_4 flow rate resulted in shorter nucleation time and more irregular graphene shapes. The layer number could also be tuned by CH_4 flow rate. We observed that the number of graphene layers decreased monotonically with the decreasing of methane flow rate in Fe-catalyzed CVD growth of FLGs.¹⁶ Moreover, the pressure and the temperature were also important in hexagonal graphene growth. Under low pressure, a continuous film or regular grains were usually obtained,^{10,14} while the formation of hexagonal graphene was only observed at a growth temperature above 900 $^\circ\text{C}$ under ambient pressure. Higher

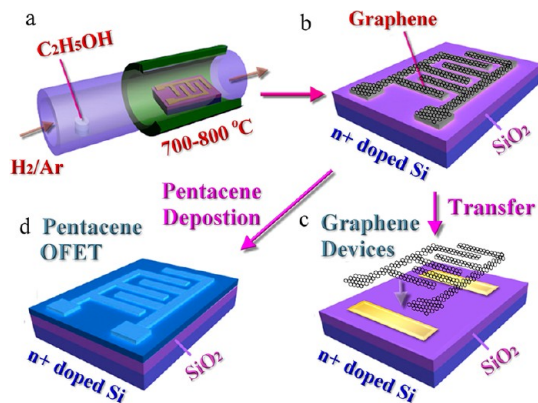


FIGURE 3. Schematic illustration of (a, b) the patterned CVD growth of graphene and its applications in (c) electric devices after transfer and in (d) source/drain electrodes of OFETs.¹⁸ Copyright 2008 Wiley Publishers.

temperature produced graphene flakes with lower density and larger size. Besides hexagonal graphene, we also observed a few hybrid FLG structures stacked by several hexagonal graphenes (Figure 2c,d). Two types of layer stacking configurations were observed with orientations either aligned or rotated by 30°. To further detail our efforts in controllable CVD growth of FLGs, the following sections will introduce several modified CVD techniques.

2.3. Patterned Growth of Few-Layer Graphene by Chemical Vapor Deposition. To fabricate devices, graphene samples need to be placed at certain locations with desired geometries. Compared with conventional lithography patterning,² patterned CVD provides a relatively simple and feasible route to achieve this goal. It relies on the feature that the epitaxial CVD growth takes place normally only on the surface of catalysts. Utilization of catalyst patterns in CVD results in the growth of graphene patterns in catalyst areas with the same shapes. For instance, as early as 2008, we placed the SiO₂/Si substrate with Cu or Ag patterns in the furnace (Figure 3a).¹⁸ After ethanol-CVD growth at 700–800 °C, FLG layers were obtained only on the Cu or Ag patterns (Figure 3b). One short-coming of this technique is the existence of catalyst metals or masks. Thus, after growth, post-treatment is usually required (Figure 3c), which partly offsets the advantages of this technique in various applications. However, this patterned graphene/metal hybrid structure shows great potential for the use of electrodes in organic semiconductor devices without post-treatment (Figure 3d), which will be detailed herein.¹⁸

2.4. Doping Few-Layer Graphene by Chemical Vapor Deposition. Doping is not only an effective approach to tailor the electronic properties of graphene, but also a

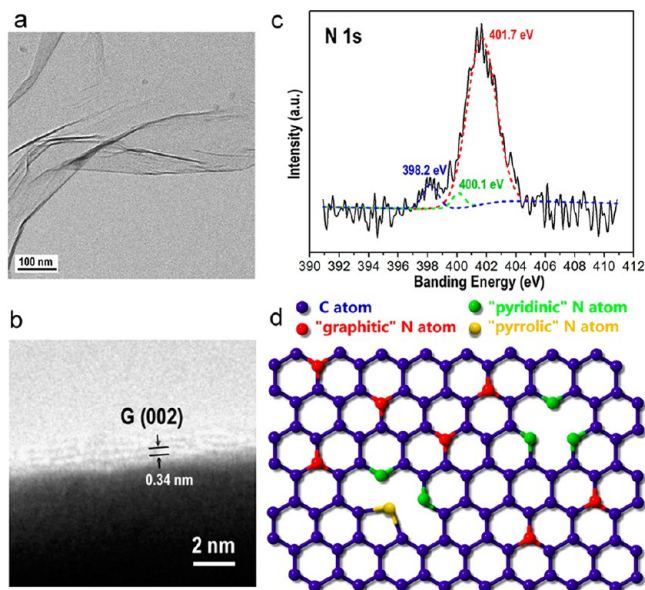


FIGURE 4. (a, b) TEM images, (c) XPS N 1s spectrum, and (d) schematic representation of the nitrogen-doped graphene. The N 1s peak in panel c can be split to three Lorentzian peaks at 401.7, 400.1, and 398.2 eV, which correspond to “graphitic”, “pyridinic”, and “pyrrolic” nitrogen, respectively, as shown in panel d. Reproduced from ref 22. Copyright 2009 American Chemical Society.

necessary technology in future graphene-based electronics, because both p-type and n-type samples are desired to construct complex logic circuits.¹⁹ There are two means to dope graphene, which are interstitial doping and substitutional doping. In the case of substitutional doping, the dopant atoms substitute the carbon atoms and bond chemically in the graphene lattice; thus it is predicted to be more stable and reliable for applications. CVD has become one of the most successful methods for substitutional doping of graphene, because it can be realized in a controllable manner simultaneously within the growth, avoiding destruction of graphene and complicated post-treatments like plasma modification²⁰ or thermal or electrical annealing in dopant gas.²¹ In 2009, we demonstrated the production of nitrogen-doped FLGs (Figure 4a) by introducing NH₃ as the nitrogen precursor in the methane CVD growth of graphene on Cu.²² In the growth, the precipitation of nitrogen atoms accompanied the formation of the graphene lattice; thus the nitrogen atoms were substitutionally doped without the destruction of the graphene lattice. Transmission electron microscopy (TEM) images (Figure 4b) showed that the products were FLGs with curved, interrupted graphitic layers. This layer morphology was also found in case of nitrogen-doped nanotubes and would be attributed to the nitrogen substitution.¹³ X-ray photoelectron spectroscopy (XPS)

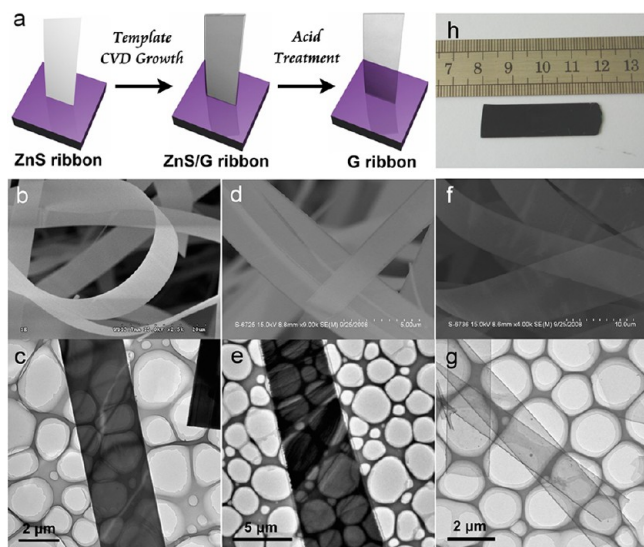


FIGURE 5. (a) Schematic diagram of the template CVD of FLG ribbons. First, ZnS ribbon arrays were prepared on a Si substrate by physical vapor deposition. Second, FLG layers were deposited on the surface of ZnS ribbons by methane CVD. Finally, after removing ZnS by HCl treatment, FLG ribbon arrays were obtained. (b–g) SEM images (b, d, f) and TEM images (c, e, g) of the ZnS ribbons (b, c), the ZnS/graphene ribbons (d, e) and the FLG ribbons (f, g). (h) Photo image of the FLG arrays grown on the Si substrate. Reproduced from ref 25. Copyright 2009 American Chemical Society.

characterization (Figure 4c) showed that the nitrogen content in the FLG was as high as 8.9 atom % ($\text{NH}_3/\text{CH}_4 = 1:1$), and nitrogen atoms were inserted into the graphene lattice in three bonding types, namely, “graphitic” (~92%), “pyridinic” (~5%), and “pyrrolic” (~3%) nitrogen (Figure 4d), and “graphitic” nitrogen was dominant. It is worth mentioning that, in 2011, scanning tunneling microscope (STM) studies by Zhao et al. observed individual nitrogen dopants in the lattice of CVD nitrogen-doped graphene that were homogeneously in the form of “graphitic” nitrogen.²³ Moreover, the nitrogen doping concentration can be modulated by the ratio of NH_3 and CH_4 in the feedstock. With lower NH_3/CH_4 ratios of 1:2 and 1:4, the nitrogen content reduced to 3.2 and 1.2 atom %, respectively. Besides nitrogen, CVD also has the potential to produce the graphene doped with other elements. For instance, recently, Li et al. synthesized boron-doped FLGs by using boron powder as the precursor in ethanol CVD growth of graphene.²⁴

2.5. Template Growth of Few-Layer Graphene by Chemical Vapor Deposition. Template CVD is a widely used and well-developed technique to produce various types of nanomaterials with controllable morphologies. We used ZnS ribbons as the template in methane CVD growth of graphene (Figure 5).²⁵ In the growth, ZnS catalyzed the growth

of FLG on the surface; thus with accompanying the carbon precipitation, the catalyst surface shapes the resulting graphene according to its surface morphology. After removing ZnS by acid treatment, FLG ribbons with shapes well-defined by the ZnS templates were obtained. Besides the shapes, the thickness of the FLG ribbons was also controllable by the growth time and the flow rate of CH_4 . Besides the morphology control, the other benefit of this technique is its scalability. Conventional CVD can produce large-area graphene with size up to wafer scale; however further scaling to bulk scale is limited in success due to the limited surface of the catalyst. High-density ZnS ribbon arrays provide a large surface area for graphene growth; thus scalable growth was realized, resulting in high density arrays of FLG ribbons on the whole surface of the Si substrate as shown in Figure 5h. Besides the ZnS ribbons, Ni nanowires²⁶ and ZnO nanowires²⁷ were also used in template growth recently, and a 3D macroscopic structure of a FLG with a foam-like network was produced by template CVD of graphene on Ni foam.²⁸

2.6. Metal-Catalyst-Free Chemical Vapor Deposition of Polycrystalline Graphene. For most applications, CVD graphene needs to be released from catalyst surface and then transferred to other substrates required in device fabrication; thus complicated and skilled postgrowth techniques are employed, which result in contamination, wrinkling, and breakage of the samples. A metal-catalyst-free CVD can avoid these short-comings. We used bare SiO_2/Si as the substrate, which was annealed at 800 °C in flowing air to activate and increase the graphene nucleation sites in the subsequent CVD growth.²⁹ After exposure to the $\text{CH}_4/\text{H}_2/\text{Ar}$ mixture gas at 1100 °C for 3 h, substrates became covered with monolayer graphene islands. After 7 h growth, continued deposition enlarged the size of graphene grains and linked the neighbor grains together, resulting in 2D interconnected polycrystalline FLGs. Detailed studies (Figure 6a,b) in TEM, STM, XPS, and Raman revealed the relatively high quality of the sample, despite no metal being employed during the growth. Besides SiO_2/Si , we also grew polycrystalline FLG films on quartz. Both the transmittance and conductivity of the films can be controlled by the growth time (Figure 6c). The films exhibited lower sheet resistance compared with chemically reduced graphene oxide,³⁰ Ni-catalyzed graphene,¹⁵ and catalyst-free nanographene³¹ and close sheet resistance to wet-transferred graphene³² with comparable transmittance, indicating the potential worth of catalyst-free CVD in the application of transparent conductivity electrodes.

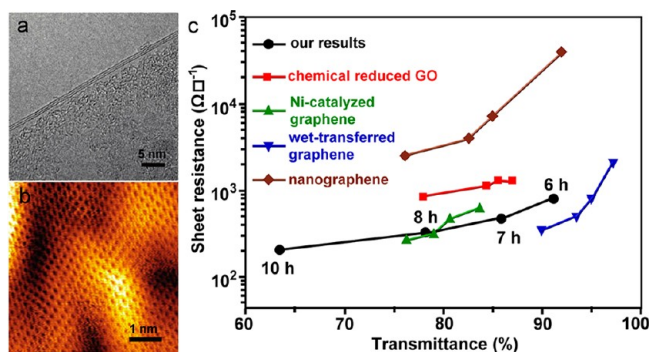


FIGURE 6. (a) HRTEM and (b) STM images of FLG directly grown on bare SiO_2/Si by metal-catalyst-free CVD. (c) The transmittance and sheet resistance of the FLG films grown on quartz by metal-catalyst-free CVD for 6, 7, 8, and 10 h, compared with other samples in the literature. Reproduced from ref 29. Copyright 2011 American Chemical Society.

3. Device Applications of Few-Layer Graphene

3.1. Application in Field-Effect Transistors. One of the most fascinating and investigated applications of graphene is in FETs.^{2,6} Figure 7a shows typical source–drain current (I_{ds}) vs the source–drain voltage (V_{ds}) curves of a FLG FET at different gate voltage (V_{g}). FLG was produced by methane CVD on copper. The most noticeable features of these curves are the good conductivity and the poor V_{g} dependence of I_{ds} , which should be attributed to the band structure of graphene. As we know, the electronic structure of graphene rapidly evolves with the layer number.^{11,12} Single-layer graphene and bilayer graphene are zero band gap semiconductors, while in case of FLG, a complex band structure forms with more charge carriers and notable overlapping of the conduction and valence bands, leading to larger metallic features.¹¹ Therefore, the lack of the band gap hampers the applications of graphene in FETs. Moreover, another problem of the CVD graphene is the growth defects and grain boundaries formed in the growth, because they would act as the scattering centers for charge transport, greatly decreasing the device performance.³³ The ambient mobilities of FLGs grown by CVD on Cu, as we measured, were only $300\text{--}1200\text{ cm}^2\text{ V}^{-1}\text{ s}^{-1}$,²² about 1–2 orders lower than the best results of mechanical exfoliation graphene ($1.5 \times 10^4\text{ cm}^2\text{ V}^{-1}\text{ s}^{-1}$).²

CVD offers a feasible means to improve the device performance. The CVD growth of hexagonal graphene crystals can greatly decrease the density of defects, especially the grain boundaries, resulting in an improved FET performance with mobilities higher than $1900\text{ cm}^2\text{ V}^{-1}\text{ s}^{-1}$.¹⁷ This value is still lower than that of the mechanical exfoliation samples, which would be attributed to the

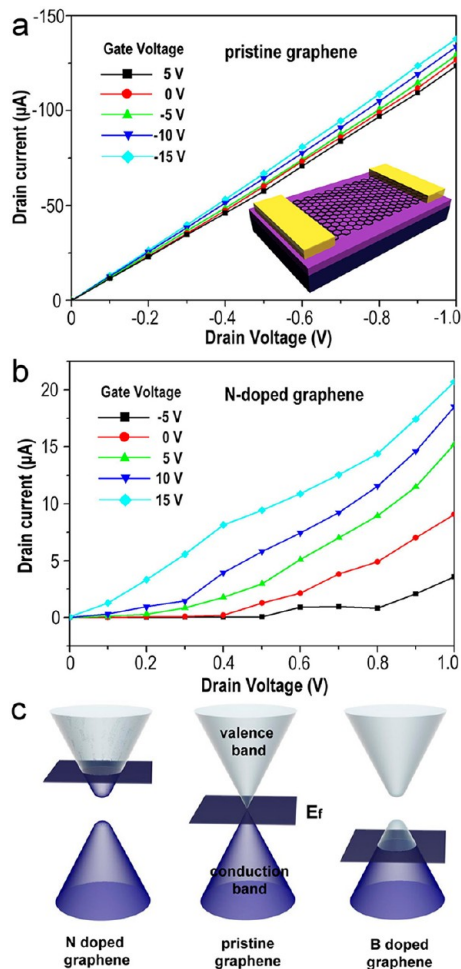


FIGURE 7. (a, b) $I_{\text{ds}}/V_{\text{ds}}$ characteristics at various V_{g} for the FETs made of pristine FLGs (a) and nitrogen-doped FLGs (b). Adapted from ref 22. Copyright 2009 American Chemical Society. (c) The presumed band structures of pristine, nitrogen-doped, and boron-doped graphene.

presence of impurities and defects introduced in PMMA-assisted transfer process. The metal-catalyst-free CVD realizes growth of polycrystalline graphene films on the dielectric surface, which can be directly used for device fabrication, avoiding the undesired transfer process. As a result, a relatively high mobility of $\sim 500\text{ cm}^2\text{ V}^{-1}\text{ s}^{-1}$ is achieved, which is better than that obtained using chemically reduced graphene oxide films or PMMA-derived graphene on Cu.²⁹

The other benefit of CVD is that it provides controllable ways to modulate the properties of the graphene samples for required FET characteristic or features. For instance, the FETs made of nitrogen-doped FLGs by CVD (Figure 7b) revealed a distinct feature compared with FETs made of pristine FLGs. An n-type behavior and an obviously improved on/off ratio (up to near 10^3 at V_{ds} of 0.5 V as V_{g} changes from -20 to 20 V) were observed with mobilities

about $200\text{--}450\text{ cm}^2\text{ V}^{-1}\text{ s}^{-1}$.²² The improved on/off ratio was also observed recently by Tang et al. in case of boron-doped graphene, which showed a p-type behavior.²⁰ Compared with carbon, the nitrogen atom has one extra electron and boron lacks one; thus the substituted nitrogen atoms donate electrons into graphene and drive an upshift of Fermi energy (E_f) level above the Dirac points, leading to n-type doping, whereas the boron results in a p-type doping (Figure 7c). Both STM and angle-resolved photoemission spectroscopy (ARPES) characteristic of the CVD nitrogen-doped graphene confirm the doping effect. Li et al. and Usachov et al. found that 50–70% of extra electrons of nitrogen dopant were delocalized into the graphene lattice,²⁴ causing an E_f upshift of 300 meV.³⁴ More importantly, as predicted in theory, the dopant atoms change the lattice structure of graphene, which largely suppress the density of states of graphene near E_f , resulting in a band gap opening.^{20,35} And the band gap is about 0.2 eV in case of CVD graphene with 0.4 atom % nitrogen dopants, according to the ARPES results.³⁴

3.2. Application as Electrodes in Organic Field-Effect Transistors. In conventional organic FETs (OFETs), the contact between the organic molecules and metal electrodes is generally poor. Graphene, to a certain degree, can be regarded as a macroscopic organic molecule with a similar structure to many organic semiconductors. Strong $\pi\text{--}\pi$ interactions are expected between them, which offer graphene great potential for applications in organic devices. We modified the surface of the Ag or Cu with FLGs by patterned CVD and used them as the bottom source/drain electrodes in OFETs by thermally evaporating 50 nm pentacene.¹⁸ Because the growth of graphene only took place on the metal electrodes, patterned CVD modified the metal electrodes without shortage in the channel. The strong interaction between graphene and pentacene resulted in the pentacene molecules lying flat on the electrode, forming a buffer surface for subsequent molecule packing (Figure 8a). A larger grain size of pentacene domains was observed on graphene compared with that on SiO_2 (Figure 8b). We even observed some pentacene crystals across the graphene/channel interface, which led to improved electrode/pentacene contact. On the other hand, the previous theoretical and experimental work showed that the graphitic materials had a work function in the 4.4–5.2 eV range,³⁶ which might result in a lower hole-injection barrier at the electrode/pentacene surface. Therefore, a dramatic reduction of contact resistance was achieved. As we measured, the graphene-modified electrodes exhibited contact resistance of 0.16–0.18 M Ω ,

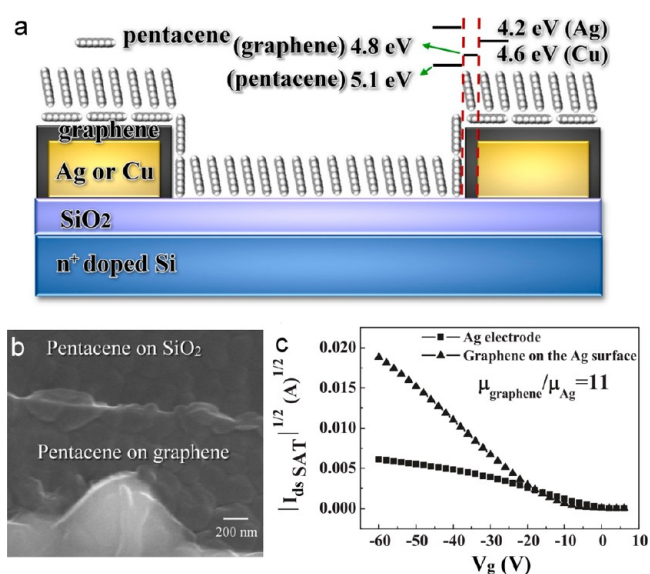


FIGURE 8. (a) Packing model of the pentacene molecules in the pentacene OFET with graphene-modified electrodes and the energy structure at the pentacene/electrode interface. (b) SEM image of a pentacene OFET at the interface of graphene-modified electrodes and SiO_2 . (c) Transfer characteristics of pentacene OFETs with graphene-modified and bare Ag electrodes. Reproduced from ref 18. Copyright 2008 Wiley Publishers.

about 1 order of magnitude lower than that of Cu or Ag electrode. More importantly, the reduced contact resistance led to a dramatically improved performance (Figure 8c) with mobilities higher than $0.5\text{ cm}^2\text{ V}^{-1}\text{ s}^{-1}$. By carefully controlling the CVD process and the pentacene deposition, field-effect mobility even up to $1.2\text{ cm}^2\text{ V}^{-1}\text{ s}^{-1}$ was achieved for pentacene-based OFETs with graphene/Au bottom electrodes and channel length of $5\text{ }\mu\text{m}$, which should be one of the best results for OFETs with bottom-contact configuration and narrow channel length.³⁷ Therefore, patterned CVD provides a simple way to modify the metal electrodes with high-quality graphene layers for high-performance organic devices. In contrast, we used inkjet printing to pattern graphene oxide solutions as the bottom source/drain electrodes for pentacene-based OFETs.³⁸ A lower mobility (about $0.2\text{ cm}^2\text{ V}^{-1}\text{ s}^{-1}$) was measured, which would be attributed to the relatively lower quality compared with CVD graphene.

3.3. Application in Electromechanical Switching Devices. One significant potential application of graphene is in nanoelectromechanics (NEM), because graphene not only shows excellent electronic properties but also has atomic thickness, large surface area, low mass density, high stiffness, and enormous strength.³⁹ The NEM switches were fabricated by current breakdown of the FLG ribbons grown

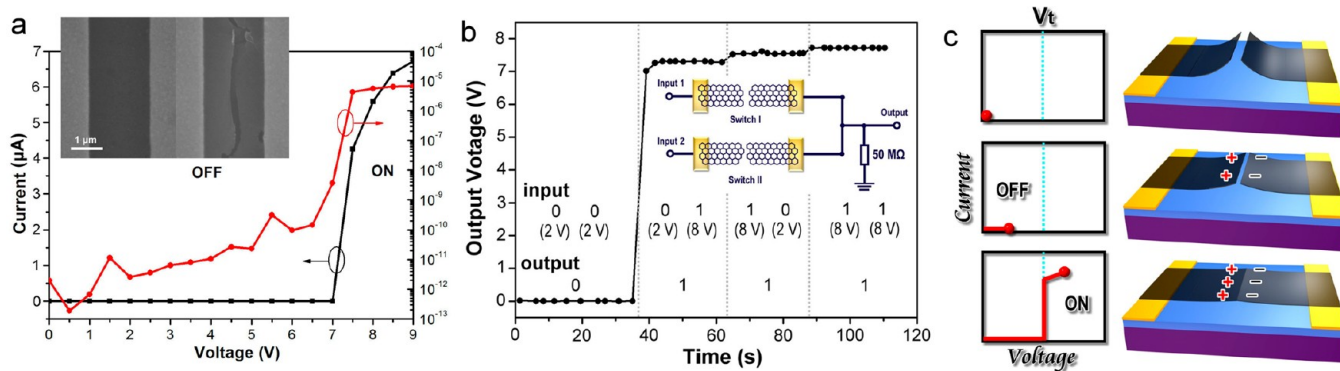


FIGURE 9. (a) I – V curves of a NEM switch made of FLG ribbons. Inset shows the SEM images of the FLG ribbon before (left) and after (right) current breakdown. (b) Output voltage of a logic OR gate made of FLG NEM switches for the four possible inputs: (0,0), (0,1), (1,0), and (1,1). Inset is the schematic of the electronic circuit of the logic OR gate. (c) The proposed switching mechanism of the NEM switch based on FLG ribbons. Adapted from ref 25. Copyright 2009 American Chemical Society.

by template CVD.²⁵ The SEM image reveals a long, narrow nanogap with curled fracture faces formed after current breakdown. Figure 9a shows typical I – V curves of the device after current breakdown, which resembles that of a bias-dependent switch. At low bias region, the current is very low, about 10^{-13} – 10^{-9} A, corresponding to the “OFF” state; the current sharply increases by about 4 orders of magnitude to 4×10^{-6} A, when the bias increases over a threshold voltage (V_t), corresponding to the “ON” state. We repeatedly cycled the bias of a FLGR switch below and above V_t , and a good reversible switching behavior was observed with an on/off ratio of about 10^{-9} . Moreover, we fabricated logic OR gate circuits by connecting two NEM switches in parallel (Figure 9b).

The long, narrow nanogap should be responsible for the reversible switching behavior (Figure 9c). This configuration can be regarded as a nanoscale capacitor with air dielectric. When a bias is applied across the gap, opposite electrostatic charges are induced on the opposite edges, giving rise to an electrostatic attractive force to deflect them toward each other. At the bias above V_t , a large electrostatic attractive force deflects the edges and causes them make electrical contact, establishing an “ON” state; while below V_t , the small electrostatic attractive force and van der Waals force cannot counteract the elastic repulsive force of the tensioned ribbon; thus the edges spring back to noncontact “OFF” state. FLGs are ideal for use of the NEM switches. It has not only a good conductivity and flexibility but also a sufficient bending rigidity for the switching operation, because the bending rigidity has a strong thickness dependence.⁴⁰

4. Conclusions

Controllable synthesis is of great significance for both fundamental research and practical applications of graphene.

In this Account, we survey our recent progress in controllable CVD growth of graphene, especially FLG, for device applications. Despite remarkable advances being achieved recently, both opportunities and challenges still remain. For instance, CVD proves a great success in controllably producing carbon nanotubes, a rolled graphene structure with nanometer-scale diameters; however how to produce sub-10 nm nanoribbons by CVD still remains a problem, and the control over the shape, edge, and doping of graphene are still limited in success at nanometer-scale. Although wafer-scale growth of graphene has been achieved by CVD, the products are still polycrystalline films with considerable growth defects and grain boundaries. It is worth noting that, recently, the CVD growth of defect-free graphene crystals has reached $10^2 \mu\text{m}$ -scale on copper or platinum,^{41,42} however more efforts are still needed to further scale up to wafer scale. This, as well as the high growth temperature and the complex postgrowth transfer process hamper actual applications of CVD graphene in electronics, at least under the present states. Anyway, CVD is one of the most promising routes to produce graphene for various applications, and there is, we believe, a bright future for the controllable CVD growth of graphene after further exploration.

We thank Professor Daoben Zhu for his long-term support. We also thank our collaborators and graduate students (past and present) who contributed to the work summarized in this Account. We acknowledge financial support from the National Basic Research Program of China (Grants 2011CB932700, 2011CB808403, and 2011CB932303), the National Natural Science Foundation of China (Grants 61171054, 20973184, 20825208, 60911130231, and 21021091), and the Chinese Academy of Sciences. Dacheng Wei acknowledges the financial

support from Lee Kuan Yew Post-Doctoral Fellowship Grant (No. R-144-000-263-112).

BIOGRAPHICAL INFORMATION

Dacheng Wei received his B.S. from Zhejiang University in 2003 and his Ph.D. from the Institute of Chemistry, CAS, in 2009. Presently, he is a Lee Kuan Yew Postdoctoral Fellow in National University of Singapore. His research work includes synthesis and applications of carbon nanotubes and graphene.

Bin Wu obtained his B.S. in 1994 from Inner Mongolia University, China, and his Ph.D. in physical chemistry from Peking University in 2002. He joined the Institute of Chemistry, CAS, as an associate professor in 2008. His research interests include mechanical properties of nanowire systems, diamondoids, the controlled growth of graphene and single-walled carbon nanotubes, and nanodevices.

Yunlong Guo received his B.S. degree in chemistry from Hebei Normal University (2005) and received his Ph.D. in chemistry from the Institute of Chemistry, CAS (2010). He was appointed as Assistant Professor in 2010. His research interest includes fabrication, characterization, and optimization of OFETs and functional OFETs.

Gui Yu graduated from Jilin University in 1988 and received his M.S. (1993) and Ph.D. (1997) degrees from Changchun Institute of Physics, CAS. After completing his Ph.D., he went to the Institute of Chemistry, CAS, as a postdoctoral associate and was appointed as professor in 2007. His research interests focus on synthesis, structures, electronic and optical properties, and theoretical investigation of novel organic semiconductors.

Yunqi Liu graduated from Nanjing University in 1975 and received a doctorate from Tokyo Institute of Technology, Japan, in 1991. Presently, he is a Professor at the Institute of Chemistry, CAS. His research interests include molecular materials and devices, the synthesis and applications of carbon nanomaterials, and organic electronics.

FOOTNOTES

*To whom correspondence should be addressed. E-mail: liuyq@iccas.ac.cn. The authors declare no competing financial interest.

REFERENCES

- Geim, A. K.; Novoselov, K. S. The rise of graphene. *Nat. Mater.* **2007**, *6*, 183–191.
- Novoselov, K. S.; Geim, A. K.; Morozov, S. V.; Jiang, D.; Zhang, Y.; Dubonos, S. V.; Grigorieva, I. V.; Firsov, A. A. Electric field effect in atomically thin carbon films. *Science* **2004**, *306*, 666–669.
- Singh, V.; Joung, D.; Zhai, L.; Das, S.; Khondaker, S. I.; Seal, S. Graphene based materials: Past, present and future. *Prog. Mater. Sci.* **2011**, *56*, 1178–1271.
- Choi, W.; Lahiri, I.; Seelaboyina, R.; Kang, Y. S. Synthesis of graphene and its applications: A review. *Crit. Rev. Solid State Mater. Sci.* **2010**, *35*, 52–71.
- Katsnelson, M. I. Graphene: Carbon in two dimensions. *Mater. Today* **2007**, *10*, 20–27.
- Schwierz, F. Graphene transistors. *Nat. Nanotechnol.* **2010**, *5*, 487–496.
- Du, X.; Skachko, I.; Barker, A.; Andrei, E. Y. Approaching ballistic transport in suspended graphene. *Nat. Nanotechnol.* **2008**, *3*, 491–495.
- Guo, Y.; Wu, B.; Liu, H.; Ma, Y.; Yang, Y.; Zheng, J.; Yu, G.; Liu, Y. Q. Electrical assembly and reduction of graphene oxide in a single solution step for use in flexible sensors. *Adv. Mater.* **2011**, *23*, 4626–4630.
- Wei, D. C.; Liu, Y. Q. Controllable synthesis of graphene and its applications. *Adv. Mater.* **2010**, *22*, 3225–3241.
- Mattevi, C.; Kim, H.; Chhowalla, M. A review of chemical vapor deposition of graphene on copper. *J. Mater. Chem.* **2011**, *21*, 3324–3334.
- Russo, S.; Craciun, M. F.; Khodkov, T.; Koshino, M.; Yamamoto, M.; Tarucha, S. Electronic transport properties of few-layer graphene materials. In *Graphene - Synthesis, Characterization, Properties and Applications*; Gong, J. R., Eds.; Intech: Shanghai, China, 2011; Chapter 9.
- Partoens, B.; Peeters, F. M. From graphene to graphite: Electronic structure around the K point. *Phys. Rev. B* **2004**, *74*, No. 075404.
- Wei, D. C.; Liu, Y. Q.; Chao, L.; Fu, L.; Li, X.; Wang, Y.; Yu, G.; Zhu, D. B. A new method to synthesize complicated multibranch carbon nanotubes with controlled architecture and composition. *Nano Lett.* **2006**, *6*, 186–192.
- Li, X.; Cai, W.; An, J.; Kim, S.; Nah, J.; Yang, D.; Piner, R.; Velamakanni, A.; Jung, I.; Tutuc, E.; Banerjee, S.; Colombo, L.; Ruoff, R. S. Large-area synthesis of high-quality and uniform graphene films on copper foils. *Science* **2009**, *324*, 1312–1314.
- Kim, K. S.; Zhao, Y.; Jang, H.; Lee, S. Y.; Kim, J. M.; Kim, K. S.; Ahn, J.-H.; Kim, P.; Choi, J.-Y.; Hong, B. H. Large-scale pattern growth of graphene films for stretchable transparent electrodes. *Nature* **2009**, *457*, 706–710.
- Xue, Y.; Wu, B.; Guo, Y.; Huang, L.; Jiang, L.; Chen, J. Y.; Geng, D.; Liu, Y. Q.; Hu, W.; Yu, G. Synthesis of large-area, few-layer graphene on iron foil by chemical vapor deposition. *Nano Res.* **2011**, *4*, 1208–1214.
- Wu, B.; Geng, D.; Guo, Y.; Huang, L.; Xue, Y.; Zheng, J.; Chen, J.; Yu, G.; Liu, Y. Q.; Jiang, L.; Hu, W. P. Equiangular hexagon-shape-controlled synthesis of graphene on copper surface. *Adv. Mater.* **2011**, *23*, 3522–3525.
- Di, C. A.; Wei, D. C.; Yu, G.; Liu, Y. Q.; Guo, Y.; Zhu, D. B. Patterned graphene as source/drain electrodes for bottom-contact organic field-effect transistors. *Adv. Mater.* **2008**, *20*, 3289–3293.
- Liu, H. T.; Liu, Y. Q.; Zhu, D. B. Chemical doping of graphene. *J. Mater. Chem.* **2011**, *21*, 3335–3345.
- Tang, Y.; Yin, L.; Yang, Y.; Bo, X.; Cao, Y.; Wang, H.; Zhang, W.; Bello, I.; Lee, S.; Cheng, H.; Lee, C. Tunable band gaps and p-type transport properties of boron-doped graphenes by controllable ion doping using reactive microwave plasma. *ACS Nano* **2012**, *6*, 1970–1978.
- Wang, X.; Li, X.; Zhang, L.; Yoon, Y.; Weber, P. K.; Wang, H.; Guo, J.; Dai, H. N-doping of graphene through electrothermal reactions with ammonia. *Science* **2009**, *324*, 768–771.
- Wei, D. C.; Liu, Y. Q.; Wang, Y.; Zhang, H.; Huang, L.; Yu, G. Synthesis of N-doped graphene by chemical vapor deposition and its electrical properties. *Nano Lett.* **2009**, *9*, 1752–1758.
- Zhao, L.; He, R.; Rim, K.; Schiros, T.; Kim, K. S.; Zhou, H.; Gutierrez, C.; Chockalingam, S. P.; Arguello, C. J.; Palova, L.; Nordlund, D.; Hybertsen, M. S.; Reichman, D. R.; Heinz, T. F.; Kim, P.; Pinczuk, A.; Flynn, G. W.; Pasupathy, A. N. Visualizing individual nitrogen dopants in monolayer graphene. *Science* **2011**, *333*, 999–1003.
- Li, X.; Fan, L. L.; Li, Z.; Wang, K.; Zhong, M.; Wei, J.; Wu, D.; Zhu, H. Boron doping of graphene through graphene-silicon p-n junction solar cells. *Adv. Energy Mater.* **2012**, *2*, 425–429.
- Wei, D. C.; Liu, Y. Q.; Zhang, H. L.; Huang, L. P.; Wu, B.; Chen, J. Y.; Yu, G. Scalable synthesis of few-layer graphene ribbons with controlled morphologies by a template method and their applications in nanoelectromechanical switches. *J. Am. Chem. Soc.* **2009**, *131*, 11147–11154.
- Wang, R.; Hao, Y.; Wang, Z.; Gong, H.; Thong, J. Large-diameter graphene nanotubes synthesized using Ni nanowire templates. *Nano Lett.* **2010**, *10*, 4844–4850.
- Xiao, T.; Heng, B.; Hu, X.; Tang, Y. In situ CVD synthesis of wrinkled scale-like carbon arrays on ZnO template and their use to supercapacitors. *J. Phys. Chem. C* **2011**, *115*, 25155–25159.
- Chen, Z.; Ren, W.; Gao, L.; Liu, B.; Pei, S.; Cheng, H.-M. Three-dimensional flexible and conductive interconnected graphene networks grown by chemical vapour deposition. *Nat. Mater.* **2011**, *10*, 424–428.
- Chen, J.; Wen, Y.; Guo, Y.; Wu, B.; Huang, L.; Xue, Y.; Geng, D.; Wang, D.; Yu, G.; Liu, Y. Q. Oxygen-aided synthesis of polycrystalline graphene on silicon dioxide substrates. *J. Am. Chem. Soc.* **2011**, *133*, 17548–17551.
- Zhao, J.; Pei, S.; Ren, W.; Gao, L.; Cheng, H.-M. Efficient preparation of large-area graphene oxide sheets for transparent conductive films. *ACS Nano* **2010**, *4*, 5245–5252.
- Zhang, L.; Shi, Z.; Wang, Y.; Yang, R.; Shi, D.; Zhang, G. Catalyst-free growth of nanographene film on various substrates. *Nano Res.* **2011**, *4*, 315–321.
- Li, X.; Zhu, Y.; Cai, W.; Borysiak, M.; Han, B.; Chen, D.; Piner, R. D.; Colombo, L.; Ruoff, R. S. Transfer of large-area graphene films for high-performance transparent conductive electrodes. *Nano Lett.* **2009**, *9*, 4259–4363.
- Chen, J.-H.; Cullen, W. G.; Jang, C.; Fuhrer, M.; Williams, E. Defect scattering in graphene. *Phys. Rev. Lett.* **2009**, *102*, No. 236805.
- Usachov, D.; Vilkov, O.; Gruneis, A.; Haberer, D.; Fedorov, A.; Adamchuk, V. K.; Preobrajenski, A. B.; Dudin, P.; Barinov, A.; Oehzelt, M.; Laubschat, C.; Vyalikh, D. V. Nitrogen-doped graphene: Efficient growth, structure, and electronic properties. *Nano Lett.* **2011**, *11*, 5401–5407.
- Martins, T. B.; Miwa, R. H.; Silva, A. J. R.; Fazio, A. Electronic and transport properties of boron-doped graphene nanoribbons. *Phys. Rev. Lett.* **2007**, *98*, No. 196803.
- Ooi, N.; Rairkar, A.; Adams, J. B. Density functional study of graphite bulk and surface properties. *Carbon* **2006**, *44*, 231–242.

- 37 Di, C. A.; Liu, Y. Q.; Yu, G.; Zhu, D. B. Interface engineering: An effective approach toward high-performance organic field-effect transistors. *Acc. Chem. Res.* **2009**, *42*, 1573–1583.
- 38 Zhang, L.; Liu, H.; Zhao, Y.; Sun, X.; Wen, Y.; Guo, Y.; Gao, X.; Di, C. A.; Yu, G.; Liu, Y. Q. Inkjet printing high-resolution, large-area graphene patterns by coffee-ring lithography. *Adv. Mater.* **2012**, *24*, 436–440.
- 39 Bunch, J. S.; Zande, A. M.; Verbridge, S. S.; Frank, I. W.; Tanenbaum, D. M.; Parpia, J. M.; Craighead, H. G.; McEuen, P. L. Electromechanical resonators from graphene sheets. *Science* **2007**, *315*, 490–493.
- 40 Poot, M.; van der Zant, H. S. Nanomechanical properties of few-layer graphene membranes. *Appl. Phys. Lett.* **2008**, *92*, No. 063111.
- 41 Li, X.; Magnuson, C.; Venugopal, A.; Tromp, R.; Hannon, J.; Vogel, E. M.; Colombo, L.; Ruoff, R. S. Large-area graphene single crystals grown by low-pressure chemical vapor deposition of methane on copper. *J. Am. Chem. Soc.* **2011**, *133*, 2816–2819.
- 42 Gao, L.; Ren, W.; Xu, H.; Jin, L.; Wang, Z.; Ma, T.; Ma, L.-P.; Zhang, Z.; Fu, Q.; Peng, L.-M.; Bao, X.; Cheng, H.-M. Repeated growth and bubbling transfer of graphene with millimetre-size single-crystal grains using platinum. *Nat. Commun.* **2012**, *3*, 699.